NIH Public Access
Author Manuscript
J Chem Neuroanat. Author manuscript; available in PMC 2010 February 1.

Published in final edited form as:
J Chem Neuroanat. 2009 March ; 37(2): 98–104. doi:10.1016/j.jchemneu.2008.11.001.

Impact of very old age on the expression of cervical spinal cord cell markers in rats

Paula Andrea Fontana[a], **Claudio Gustavo Barbeito**[a], **Rodolfo Gustavo Goya**[b], **Eduardo Juan Gimeno**[a], and **Enrique Leo Portiansky**[a,*]

a*Institute of Pathology, School of Veterinary Sciences, National University of La Plata (UNLP), La Plata 1900, Argentina*

b*INIBIOLP-Histology "B", School of Medicine, National University of La Plata, La Plata 1900, Argentina*

Abstract

Aging is a process associated with both anatomical changes and loss of expression of some cell markers. Intermediate filaments are known to impart mechanical stability to cells and tissues. Some of them are present in different cell populations of the central nervous system. In order to explore the impact of extreme age we immunohistochemically characterized the changes in intermediate filaments and other cellular markers present in cells populating the gray matter cervical spinal cord of very old rats (28 months) taking young (5 months) counterparts as a reference. The spinal cord weight of the senile animals (12.6 ± 1.1 g) was significantly higher ($P < 0.001$) than that of the young animals (8.4 ± 1.1 g). Spinal cord length also increased significantly ($P < 0.05$) with age (7.9 ± 0.3 cm vs. 8.28 ± 0.1 cm for young and senile, respectively). An increase in both neurofilament staining area and density was observed in senile rats in comparison to young animals. A significant ($P < 0.05$) age-related increment in the mean area of the cervical segments was observed. Vimentin expression in the ependymal zone decreased in area and intensity during aging. Our data show that there are some significant changes in the morphological and histochemical patterns of the cervical spinal cord in senile rats. However, they do not necessarily represent a pathologic situation and may rather reflect plastic reorganization.

Keywords

Intermediate filaments; Histochemistry; Morphometry

1. Introduction

Although a number of rat models for assessing morphological changes during disease and injury of the spinal cord have been described (Liu et al., 1999; Jasmin and Ohara, 2004; Anderson et al., 2007; Kalous et al., 2007), there is little information on the morphologic changes in spinal cord cells of old rats and even less in senile (>28 months of age) animals. WAGxBN 30-month-old male, but not female rats were reported to show a high prevalence of paralysis or severe paresis of the hind limbs and atrophy of the skeletal muscles in the lumbar region and hind limbs. At the microscopic level the lesions of the lumbar spinal cord were reported to be limited to the white matter and consisted of demyelination, distended axon sheaths, swollen or absent axons and numerous swollen astrocytes (Burek, 1978). We are unaware of similar studies in the cervical segments of very old rats.

*Corresponding author at: Institute of Pathology, School of Veterinary Sciences, UNLP, Calle 60 y 118, CC 296, La Plata 1900, Argentina. Tel.: +54 221 423 6663/4x426; fax: +54 221 425 7980. *E-mail address:* E-mail: elporti@fcv.unlp.edu.ar (E.L. Portiansky).

NIH-PA Author Manuscript
NIH-PA Author Manuscript
NIH-PA Author Manuscript

NIH-PA Author Manuscript

NIH-PA Author Manuscript

NIH-PA Author Manuscript

In a recent study we observed a complete loss of neuron-specific nuclear protein (NeuN) immunoreactivity in cervical, thoracic and lumbar segments of senile (32-month) female rats whereas neuron-specific enolase (NSE) immunoreactivity was comparable in young and senile animals (Portiansky et al., 2006).

Since intermediate filaments (IFs) are known to impart mechanical stability to cells and tissues and are believed to play a pivotal role in mechanotransduction (Kreplak and Fudge, 2007), it was of interest to characterize the age changes in IF of the cervical spinal cord of very old rats, as well as in other cellular markers.

2. Materials and methods

Young (5-month-old; $n = 5$) and senile (28-month-old; $n = 5$) clinically healthy Sprague–Dawley female rats were used. The weight range of the animals was 180–200 g (young) and 230–240 g (senile). The body length of the rats measured from the nose to the anus was 18 ± 0.4 and 20.5 ± 0.5 cm in young and senile animals, respectively.

Animals were anaesthetized with an i.p. injection of ketamine hydrochloride (40 mg/kg) followed by an i.m. injection of xylazine (Rompun®, Bayer; 8 mg/kg). Rats were then perfused through the left ventricle with 4% para-formaldehyde (Anedra, Argentina) solution in PBS 0.1 M, pH 7.4 during 15 min. Sacrifice of animals followed the international rules specified in the "Guidelines on the Use of Animals in Neuroscience Research (The Society of Neuroscience)" and "Research Laboratory Design Policy and Guidelines of NIH".

The spinal cord of each rat was removed and fixed in 10% buffered formalin during 48 h. The spinal cord of all animals was weighed and measured in length from the nerve eminences in the first segment to the conus medullaris.

Segments C1–C8 were either embedded in paraffin ($n = 3$ per age group) or prepared for vibratome section ($n = 2$ per age group). Ten μm sections of each paraffin embedded segment were stained either with cresyl violet for morphometric analysis or with immunohistochemical techniques for quantitative analysis. Forty-micrometer coronal sections of every cervical segment were sectioned with a vibratome, mounted on gelatine-embedded slides and stained either with cresyl violet for morphometric analysis or immunofluorescence techniques for qualitative observation.

2.1. Immunohistochemistry (IHC)

After dewaxing, sections were treated with 0.3% H_2O_2 in methanol for 30 min at room temperature, rinsed several times in 0.01 MPBS, and treated with 0.1% bovine serum albumin in PBS for 15 min. Sections were then incubated during 2 h at room temperature with the following primary antibodies: monoclonal mouse antihuman neurofilament protein (NF), clone 2F11 (DakoCytomation, Carpinteria, CA, USA). It reacts with the phosphorylated form of the 70 kDa component (the low molecular weight subunit) of the NF protein; monoclonal mouse anti-vimentin clone V9 (DakoCytomation). It recognises the IF type III 57 kDa protein, vimentin; polyclonal rabbit anti cow glial fibrillary acidic protein (GFAP) (DakoCytomation). It specifically binds to the IF protein present mainly in astrocytes and ependynal cells; rat anti-nestin (Rat-401; S Hockfield, Hybridoma Bank, University of Iowa). It recognises the IF Nestin from mouse and rat; polyclonal rabbit anti-cow S100a (prediluted, DakoCytomation, Carpinteria, CA, USA). It binds to the 20–30 kDa acidic calcium binding protein present mainly in glial cells. It reacts with both α and β subunits of the S-100 protein. The IHC detection system was a dextran polymer based method (Universal EnVision®System, DakoCytomation) and was applied according to the manufacturer's instructions. The 3,3′diaminobenzidine tetrahydrochloride (DAB) (DakoCytomation) was used as a chromogen. Those cells showing a dark

NIH-PA Author Manuscript

NIH-PA Author Manuscript

NIH-PA Author Manuscript

golden brown DAB-H_2O_2 reaction product were considered as positively stained. The same tissues but without adding the primary antibody, were used as negative controls. Haematoxylin was used for counterstaining.

For fluorescence IHC, the primary antibodies were anti-NF, anti-vimentin and anti-GFAP (Sigma) and the secondary antibodies were either Alexa488-conjugated goat anti-mouse IgG or Alexa488-conjugated goat anti-rabbit IgG (Invitrogen, USA; 1:1000). Fluorescence was detected with an Olympus BX61 epifluorescence microscope at excitation/emission wavelengths of 470/505 nm. Images were captured as monochrome and then pseudocoloured.

2.2. Morphometry

Morphometry was carried out on digital images captured through a camera (Evolution VF, QImaging, Canada) attached to a microscope (Olympus BX61, Japan) and processed using an image analysis software (ImagePro Plus, v6.3, Media Cybernetics, USA). Raw images (RGB 24 bits TIFF format) obtained from five slide sections of every cervical segment, cut at 100 μm apart were used for morphometric purposes and determination of the mean optical density (MOD) of the stained structures. Images either of the entire spinal cord section (1.25×, 4× objectives) or hemisections for each tested antibody were analysed. The amount of marker present in different peroxidase stained structures and cells of the analysed spinal cord segments was determined by comparing the MOD of the positive reaction against a negative control. For doing so, all the samples corresponding to the same analysed protein were processed in the same day. Moreover, all images corresponding to the same protein were captured with the same microscope and camera parameters. Images were then processed by the image analysis software for background correction. Background correction is achieved by obtaining an image of the light of the microscope passing through the microscope slide, the mounting media (synthetic Canada balsam—Biopack, Argentina) and the cover slip, in a tissue-free area. Pixels deemed to be part of the background, will mathematically be replaced by the software with a value corrected for OD measurement purposes. In order to select positively stained areas (peroxidase brown stain) for further morphometric measurements, and also to separate it from the counterstained or not stained tissues sectors, the Colour Segmentation process of the image analysis program was applied. A mask was then applied to make the separation of colours permanent. Images where then converted to an 8-bit gray-scale TIFF format. After spatial and intensity of light calibration of images, the MOD of the labelled reaction was obtained.

The distribution of the IHC positively stained structures was assessed using the formula:

$$\%\text{IHCSA} = \text{stained area}/\text{total area} \times 100$$

where %IHCSA is the percentage of immunohistochemical stained area and total area refers to the structure considered (i.e. whole gray matter). The following structures were considered in the analysis: neuronal bodies, neuropil, ependymal cells and gray matter glial cells.

Gross morphometric measurements included the whole segment area and the length and width (Feret diameters) of every cervical segment were determined using a low magnification objective (1.25×).

White matter cross-sectioned axons of the ventral corticospinal tract were morphometrically analysed by means of area, mean diameter and roundness (that reports the roundness of each object, as determined by the following formula: $(\text{perimeter}^2)/(4 \times \pi \times \text{area})$. Circular objects will have a roundness = 1; other shapes will have a roundness > 1). Over 4500 randomly selected axon IHC reacting with NF of every age group were analysed. Values were expressed as mean ± S.E.

NIH-PA Author Manuscript

NIH-PA Author Manuscript

NIH-PA Author Manuscript

For determining axonal density of NF positively stained and cross-sectioned axons (range area between 0.5 and 15 μm^2), 80 square areas of 2500 μm^2 each were randomly selected from the ventral corticospinal tract of young and senile rats. Results were expressed as mean count per unit area (2500 μm^2) ± S.E.

Data obtained was exported to a spreadsheet in order to perform statistical analysis.

2.3. Statistical analysis

Morphometric data were statistically assessed by the Student's paired *t*-test. *P*-values < 0.05 were considered to indicate significant differences.

3. Results

3.1. Anatomical changes of different cervical segments during aging

Low magnification assessment of spinal cord sections corresponding to the cervical segments already revealed a clear age-related increase in the overall area (Fig. 1A–E). This increase achieved statistical significance between both age groups. The spinal cord weight of the senile animals (12.6 ± 1.1 g) was significantly higher ($P < 0.001$) than that of the young animals (8.4 ± 1.1 g). Spinal cord length also increased significantly ($P = 0.035$) with age (7.9 ± 0.3 cm vs. 8.28 ± 0.1 cm for young and senile, respectively). Nevertheless, the mean length difference between age groups was lower than the average length of individual cervical segments.

A significant age-related increment in the mean area of the cervical segments was observed. The overall cervical cross-sectional area increase with age was 15.6%, with the highest and lowest increments occurring in C3 (24.1%) and C6 (9.7%), respectively (Fig. 1C). This change was due to both gray matter and white matter increase with the former showing a greater enlargement than the latter, as indicated by the reduction in the ratio white matter:gray matter (Fig. 1F).

3.2. Expression of intermediate filaments markers in cervical segments of young and senile rats

3.2.1. NF expression during aging—IHC for NF showed an increase in the stained area as well as in NF density in the senile rats in comparison to young animals although the MOD was similar for both groups (0.53 ± 0.03 vs. 0.51 ± 0.04 young vs. senile, respectively). Such differences were significant (Fig. 2A–E). In no case NF staining was observed in laminae I and II nor in the gracile nuclei. In the other laminae NF were stained evenly.

3.2.2. GFAP expression during aging—IHC for GFAP was also performed in order to determine possible modifications of expression of this astrocytic marker with age (Fig. 3A and B). A significant increase in the GFAP stained area (area occupied by astrocyte somas and processes) was observed only in C5 segments of senile rats (Fig. 3C). Moreover, the percentage of staining with respect of the entire gray matter was inverted in the last 3 cervical segments. A highly significant decrease was observed for the MOD of this marker with age (0.58 ± 0.01 vs. 0.48 ± 0.01 young vs. senile, respectively). GFAP positive cells were uniformly distributed throughout both the gray and white matter. As expected, neither young nor senile rats showed ependymal cell staining for this marker.

3.2.3. Nestin expression in young and senile rats—This IF marker was detected in neither age group.

3.2.4. Vimentin expression during aging—Vimentin was observed in ependymal cells as well as in some glial cells and surrounding blood vessels (Fig. 4A–D) in young as well as

NIH-PA Author Manuscript

NIH-PA Author Manuscript

NIH-PA Author Manuscript

in senile rats. Nevertheless, vimentin positive cell number and labelling MOD levels significantly decreased with age (Fig. 4E). Moreover, the vimentin stained area present in senile rats decreased from C1 to C8.

3.3. Expression of other markers in cervical segments of young and senile rats

3.3.1. S100 expression during aging—The S100 marker expressed mainly in glial cells was also assessed (Fig. 5A–G). A significant increase in the number of S100 positive cells was observed in the C2 and C8 segments with the former recorded in young and the latter recorded in senile rats (Fig. 5H). No significant age-related differences were observed in the MOD of positively stained cells (Fig. 5I). S100 positive cells were uniformly distributed in both the gray and white matter. Although mainly restricted to cell bodies, positive staining was also observed in the processes of the cells. The marker was also detected in ependymal cells of both groups as well as in some of the motoneurons of both age groups. In the latter case, staining was restricted to the nuclei. In some cases, neurons of lamina VII and X showed the same pattern.

3.4. Morphometry of white matter axons

Cross-sectional area ($1.65 \pm 0.08\ \mu m^2$) and mean diameter values (1.41 ± 0.03 mm) for axons of young rats did not differ significantly from those of senile animals ($1.52 \pm 0.07\ \mu m^2$ and $1.37 \pm 0.03\ \mu m$, respectively). Age-related significant differences ($P < 0.001$) were observed in axon roundness (1.41 ± 0.01 vs. 1.29 ± 0.01, for senile and young rats, respectively).

Axonal density analysis revealed a significant increase ($P = 0.002$) in the number of axons in the ventral corticospinal tract per unit area in senile rats in comparison to young animals (87.93 ± 12.84 vs. 48.13 ± 8.79 mean axon number/$2500\ \mu m^2$, respectively).

4. Discussion

For many years the aging female Sprague–Dawley rat has been our model for studies related to brain and spinal cord aging. In the spinal cord, we have previously shown that in female rats, aging is associated with a loss of expression of both the NeuN antigen (Portiansky et al., 2006) and some carbohydrate residues (Lozza et al., in press).

The present results provide additional information about the impact of aging on spinal cord morphology, showing that aging brings about a significant sectional enlargement of the cervical spinal cord of female rats. Flynn and Bolton (2007) have recently shown that the rat cervical portion of the vertebral canal has different vertical and transverse dimensions. The authors describe an increase in transversal size from C2 to C7. The same pattern was observed in the present study in the spinal cord of senile but not young rats where a cervico-thoracic enlargement from C4 to C6 is evident.

Since no degenerative alterations of this region were observed in the senile animals it seems likely that growth of spinal cord tissue during aging may serve some functional (perhaps adaptive) purpose.

It should be mentioned that the female rat reaches growth stasis at about 4 months of age. Subsequently the gain in body weight is mainly accounted for by increase in body fat (de Heredia et al., 2008). Consequently, the increase in section size of the cervical segments does not seem to be part of body growth during aging. Moreover, 12-month-old male rats of the same strain, weighing over 100 g more than 5-month-old females have section areas of the cervical segments similar or even smaller (Portiansky et al., 2004).

NIH-PA Author Manuscript

NIH-PA Author Manuscript

NIH-PA Author Manuscript

Our results show that spinal cord size increases during the lifetime of female rats despite adult (4 months) stasis in body growth. This spinal growth is associated with an increase in the gray matter:white matter ratio. Furthermore, the data showing incremental variation of NF reflects a predominant increase in the neuropil mass with age, which seems to account, at least in part, for the observed increase in the mentioned ratio.

When analysing the axonal density based on NF stained tissues we observed an increase in the number of axons per unit area in aged rats. This is in agreement to what was observed by Uchida et al. (1999) on rat sciatic nerves and Shiozaki et al. (2008) in Klotho mutant mice. Moreover, as described by Uchida et al. (1999), there was an increase in the non-roundness of the axons in aged animals as we have observed in our study. The increase in axonal density in the senile rats offers a plausible, although not exclusive, explanation for the increase in size of their white matter.

Our data relative to markers that characterize other structures also present in the gray matter, indicate that glial and ependymal cells do not contribute significantly to the age-related increase in the gray matter:white matter ratio in the cervical spinal cord.

NF is a type IV family of intermediate filaments that is found in high concentrations along the axons of vertebrate neurons although they have also been found in spinal cord motoneurons' dendrites (Wuerker and Palay, 1969). During axonal growth, new NF subunits are incorporated along the axon in a dynamic process that involves the addition of subunits along the filament length, as well as the addition of subunits at the filament ends. After an axon has grown and connected with its target cell, the diameter of the axon may increase as much as fivefold (Alberts et al., 2002). It seems that maximum axon diameter is reached at young age since the cross-sectional area and mean diameter of the axons measured in young rats were always greater than those of senile rats, although these differences did not reach statistical significance.

It has been reported that the heavy portion of NF protein increases in pathological conditions such as amyotrophic lateral sclerosis and other human diseases like Parkinson's and Alzheimer's disease (Al-Chalabi and Miller, 2003). In most cases a spheroid formation was observed (Cairns et al., 2004). Accumulation of NF may impair the axonal transport of supplies required for axonal activity, resulting in degeneration of the distal axon and eventually of the whole neuron (Uchida et al., 1999). Nevertheless, in our work only the L subunit NF was tested and in no case signs of pathological alterations were detected. The increased expression of this same NF subunit was also observed in Klotho mutant mice, an animal model for accelerated human aging, where no morphological cellular degenerative changes were observed (Shiozaki et al., 2008).

It has been shown that in middle-aged/old mice (1–2 years) axonal atrophy occurs thus reducing the amount of NF (Elder et al., 1999). The collapse of the axons is not simply a direct result of a depleted NF number but rather a depleted NF content renders these axons more susceptible to atrophy (Sakaguchi et al., 1993). If NF deficiency leads to axon atrophy, then an increase in NF similar to that observed here should tend to prevent this atrophy.

One expected consequence of a reduced axonal diameter is a reduced nerve conduction velocity and this has been demonstrated to occur in the NF-L-deficient quail (Sakaguchi et al., 1993). In each of the diverse neuronal states from differentiation in the embryo through long-term activity in adult and old age, NF function could be modulated by phosphorylation–dephosphorylation reactions that define the nature of NF interaction with one another and with other cytoskeletal components. A generally accepted hypothesis states that NF promotes radial growth, stabilizing large caliber axons, thereby increasing conduction velocity of large myelinated fibres (Hilbig et al., 2002).

NIH-PA Author Manuscript

NIH-PA Author Manuscript

NIH-PA Author Manuscript

Whether NF increase during aging could be ascribed to age-related differences in circulating oestrogen levels in our female rats is difficult to ascertain. Although estrogen levels do change with age (tend to increase and lose cyclicity) other hormones also change with age (in both males and females), particularly prolactin which increases significantly. Therefore, a comprehensive neuroendocrine analysis correlating hormone changes with morphological changes in spinal cord NF, should be carried out in order to determine possible cause-effect relationships between age-changes in hormones and spinal cord structures. Such an analysis was beyond the scope of the present study. It is of interest to mention that Chiasson et al. (2006) have shown that NF-L mRNA is not influenced by estradiol.

While GFAP and S-100 expression was not substantially affected by aging, the significance of the loss of vimentin expression in the aged rats is not clear at present.

Vimentin is a member of the IF family of proteins that identify mesenchymal cells, primitive neuroepithelial cells, astrocytes and developing neurons (Ho and Liem, 1996). It is attached to the nucleus, endoplasmic reticulum and mitochondria, either laterally or terminally. Essentially, the protein is responsible for maintaining cell shape, integrity of the cytoplasm, and stabilizing cytoskeletal interactions (Ivaska et al., 2007). Vimentin staining was observed in ependymal cells, scattered glial cells and surrounding blood vessels. We have observed a decrease in the amount and intensity/density of staining with age. It remains to be clarified whether this decrease in vimentin levels is associated with functional changes in the aging spinal cord.

Pekny and Wilhelmsson (2007) showed that in non-reactive astrocytes, IF consist of GFAP and vimentin, while in mature astrocytes, the major protein of the IF network is GFAP, and the vimentin level ranges from very low to intermediate, depending on the subpopulation of astrocytes. We have observed vimentin mainly in the ependymal cells where the amount and intensity of this IF decreased with age in the cervical segments of the spinal cord which may reflect a decrease in the number of the above precursor cells.

In the present study we observed that no significant changes occurred in cell number or in the area occupied by glial cells. It is well established that after an insult to neurons, there is an increase in the number of glial cells, particularly microglia and astrocytes which are respectively responsible for pain generation and neuroprotective factor production (Vega-Avelaira et al., 2007). In our senile rats the lack of a significant increase in the glial populations (and lack of inflammatory foci) can be interpreted as an index of anatomical and functional normalcy concerning cervical nervous segments, despite the reported age changes. Moreover, the decrease in MOD and in the percentage of IHC stained area in the senile animals suggests a lower density of astroglial processes probably linked to the aging process but in the absence of inflammation.

Nestin is a type VI IF protein expressed mostly in nerve cells and implicated in the radial growth of the axon. It is expressed transiently during development and does not persist into adulthood. Nestin expression is reinduced in the adult during pathological situations, such as the formation of the glial scar after central nervous system injury (Guerette et al., 2007). The fact that this marker was not detected in senile rats taken together with the fact that no increase of glial cells was observed, suggests that cervical spinal cord aging is not associated with a pathological condition and that growing of the whole cervical segments and particularly of the gray matter is a physiological process.

Although a number of significant differences were found in the present study, the number of rats used per group was low. This low N may have caused that some of the nonsignificant differences reported here are small but significant and would require the use of a larger N to make them statistically evident.

NIH-PA Author Manuscript

NIH-PA Author Manuscript

NIH-PA Author Manuscript

Taken together the present data reveal a dysbalanced but seemingly nonpathological growth of cervical spinal cord components during aging in rats and shows that predominant neuropil growth contributes to the increase in the proportion of gray matter segments of old animals. Whether this phenomenon is exclusive of the cervical spinal cord or it occurs throughout the spinal cord of aged rats remains to be investigated.

Acknowledgements

This study was partially financed by grant # PICT 2006/583 from the National Agency for the Promotion of Science and Technology (ANPCyT) to ELP, grant # 11/V167, National University of La Plata and grant NIH#1 R01 AG029798 from the National Institute on Aging (NIA) to RGG and ELP. PAF, CGB, RGG, EJG and ELP are Research Career Members of CONICET (Argentinean National Scientific Research Council). Our gratitude to Mrs. Rosa illegas and Maria Guadalupe Guidi for their technical assistance.

References

Alberts, B.; Johnson, A.; Lewis, J.; Raff, M.; Roberts, K.; Walter, P. The cytoskeleton. In: Alberts, B.; Johnson, A.; Lewis, J.; Raff, M.; Roberts, K.; Walter, P., editors. Molecular Biology of the Cell. Vol. 4th ed.. USA: Garland Science; 2002. p. 907-982.

Al-Chalabi A, Miller CC. Neurofilaments and neurological disease. Bioessays 2003;25:346–355. [PubMed: 12655642]

Anderson KD, Gunawan A, Steward O. Spinal pathways involved in the control of forelimb motor function in rats. Exp. Neurol 2007;206:318–331. [PubMed: 17603042]

Burek, JD. Pathology of Aging Rats. Boca Ratón: CRC Press; 1978.

Cairns NJ, Grossman M, Arnold SE, Burn DJ, Jaros E, Perry RH, Duyckaerts C, Stankoff B, Pillon B, Skullerud K, Cruz-Sanchez FF, Bigio EH, Mackenzie IR, Gearing M, Juncos JL, Glass JD, Yokoo H, Nakazato Y, Mosaheb S, Thorpe JR, Uryu K, Lee VM, Trojanowski JQ. Clinical and neuropathologic variation in neuronal intermediate filament inclusion disease. Neurology 2004;63:1376–1384. [PubMed: 15505152]

Chiasson K, Lahaie-Collins V, Bournival J, Delapierre B, Gélinas S, Martinoli MG. Oxidative stress and 17-alpha- and 17-beta-estradiol modulate neurofilaments differently. J. Mol. Neurosci 2006;30:297–310. [PubMed: 17401155]

de Heredia FP, Larque E, Del Puy Portillo M, Canteras M, Zamora S, Garaulet M. Age-related changes in fatty acids from different adipose depots in rat and their association with adiposity and insulin. Nutrition 2008;24:1013–1022. [PubMed: 18562171]

Elder GA, Friedrich VL Jr, Margita A, Lazzarini RA. Age-related atrophy of motor axons in mice deficient in the mid-sized neurofilament subunit. J. Cell Biol 2008;146:181–192. [PubMed: 10402469]

Flynn JR, Bolton PS. Measurement of the vertebral canal dimensions of the neck of the rat with a comparison to the human. Anat. Rec 2007;290:893–899.

Guerette D, Khan PA, Savard PE, Vincent M. Molecular evolution of type VI intermediate filament proteins. BMC Evol. Biol 2007;7:164. [PubMed: 17854500]

Hilbig H, Bidmon HJ, Steingrüber S, Reinke H, Dinse HR. Enriched environmental conditions reverse age-dependent gliosis and losses of neurofilaments and extracellular matrix components but do not alter lipofuscin accumulation in the hindlimb area of the aging rat brain. J. Chem. Neuroanat 2002;23:199–209. [PubMed: 11861126]

Ho CL, Liem RK. Intermediate filaments in the nervous system: implications in cancer. Cancer Metast. Rev 1996;15:483–497.

Ivaska J, Pallari HM, Nevo J, Eriksson J. Novel functions of vimentin in cell adhesion, migration, and signaling. Exp. Cell Res 2007;313:2050–2062. [PubMed: 17512929]

Jasmin L, Ohara PT. Recurrent paraplegia after remyelination of the spinal cord. J. Neurosci. Res 2004;77:277–284. [PubMed: 15211594]

Kalous A, Osborne PB, Keast JR. Acute and chronic changes in dorsal horn innervation by primary afferents and descending supraspinal pathways after spinal cord injury. J. Comp. Neurol 2007;504:238–253. [PubMed: 17640046]

NIH-PA Author Manuscript

NIH-PA Author Manuscript

NIH-PA Author Manuscript

Kreplak L, Fudge D. Biomechanical properties of intermediate filaments: from tissues to single filaments and back. Bioessays 2007;29:26–35. [PubMed: 17187357]

Liu C, Edwards S, Gong Q, Roberts N, Blumhardt LD. Three dimensional MRI estimates of brain and spinal cord atrophy in multiple sclerosis. J. Neurol. Neurosurg. Psychiatry 1999;66:323–630. [PubMed: 10084530]

Lozza FA, Chinchilla LA, Barbeito CG, Goya RG, Gimeno EJ, Portiansky EL. Changes in carbohydrate expression in the cervical spinal cord of rats during aging. Neuropathology. in press.

Pekny, M.; Wilhelmsson, U. GFAP and astrocyte intermediate filaments. In: Lajtha, Abel; Lim, Ramon, editors. Handbook of Neurochemistry and Molecular Neurobiology. Vol. 3rd ed.. USA: Springer; 2007. p. 289-314.

Portiansky EL, Barbeito CG, Goya RG, Gimeno EJ, Zuccolilli GO. Morphometry of cervical segments grey matter in the male rat spinal cord. J. Neurosci. Methods 2004;139:217–229. [PubMed: 15488235]

Portiansky EL, Barbeito CG, Gimeno EJ, Zuccolilli GO, Goya RG. Loss of NeuN immunoreactivity in rat spinal cord neurons during aging. Exp. Neurol 2006;202:519–521. [PubMed: 16935281]

Sakaguchi T, Okada M, Kitamura T, Kawasaki K. Reduced diameter and conduction velocity of myelinated fibers in the sciatic nerve of a neurofilament-deficient mutant quail. Neurosci. Lett 1993;153:65–68. [PubMed: 8510825]

Shiozaki M, Yoshimura K, Shibata M, Koike M, Matsuura N, Uchiyama Y, Gotow T. Morphological and biochemical signs of age-related neurodegenerative changes in Klotho mutant mice. Neuroscience 2008;152:924–941. [PubMed: 18343589]

Uchida A, Yorifuji H, Lee VM, Kishimoto T, Hisanaga S. Neurofilaments of aged rats: the strengthened interneurofilament interaction and the reduced amount of NF-M. J. Neurosci. Res 1999;58:337–348. [PubMed: 10502290]

Vega-Avelaira D, Moss A, Fitzgerald M. Age-related changes in the spinal cord microglial and astrocytic response profile to nerve injury. Brain Behav. Immun 2005;21:617–623. [PubMed: 17158026]

Wuerker RB, Palay SL. Neurofilaments and microtubules in anterior horn cells of the rat. Tissue Cell 1969;1:387–402. [PubMed: 18631475]

NIH-PA Author Manuscript
NIH-PA Author Manuscript
NIH-PA Author Manuscript

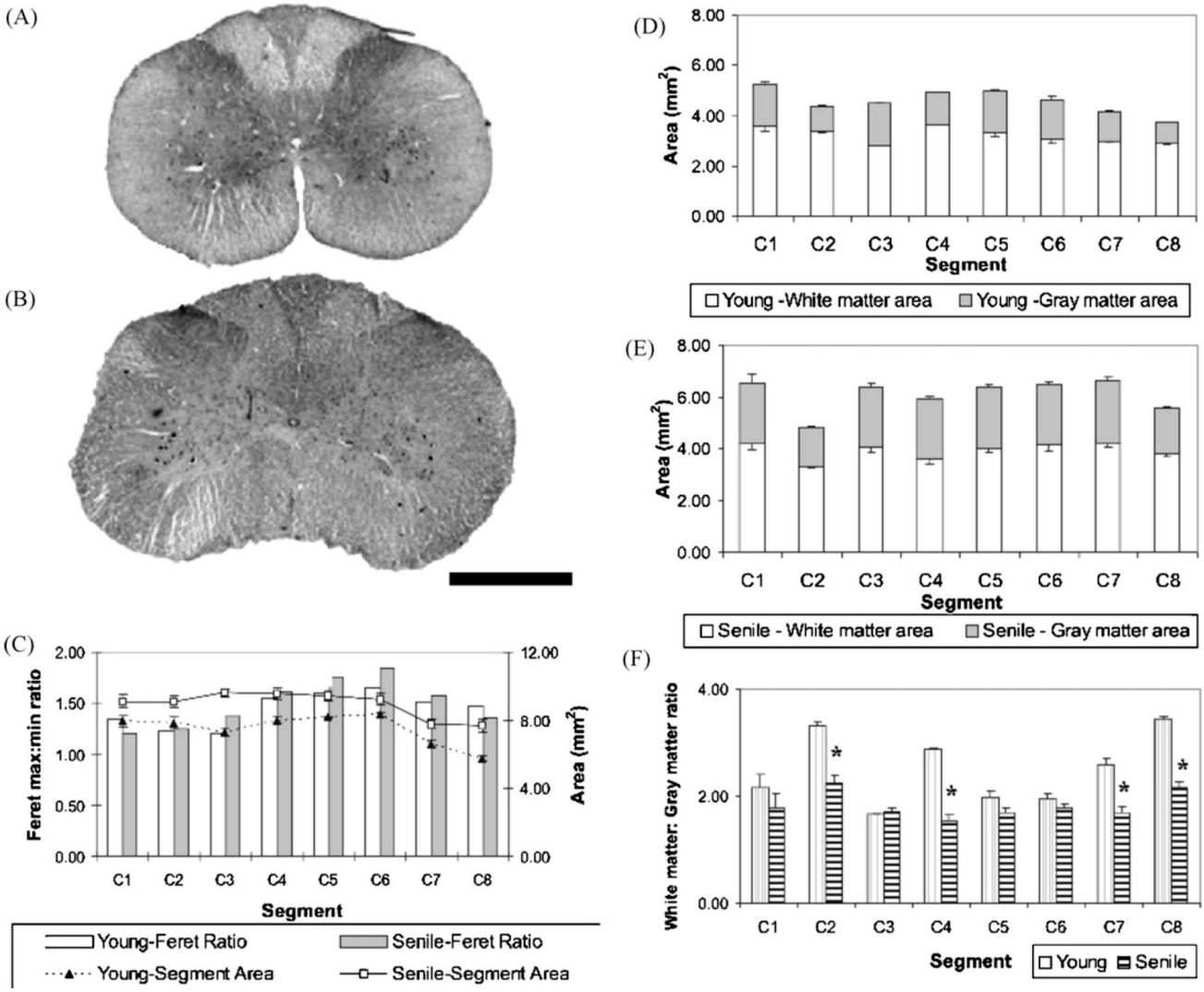

Fig. 1. Anatomical changes of different cervical segments during aging

An increase in the whole size of each cervical segment was observed during aging. C5 segments of young animals (A) ($n = 5$) showed a round shaped structure with a round central canal while senile rats (B) ($n = 5$) showed a more elongated section shape and central canal. An evident change in the gray matter ventral horn shape is also observed during aging. Such differences were also observed throughout the eight cervical segments of both analysed groups (C). In all the segments differences in whole area were significant. A significant increase in the white matter as well as in the gray matter was observed in senile rats (E) in comparison with young animals (D). Nevertheless, that increase was more pronounced in the gray matter as judge by the significant reduction in the ratio between both substances (F). *Significant difference. Bar = 1 mm.

NIH-PA Author Manuscript
NIH-PA Author Manuscript
NIH-PA Author Manuscript

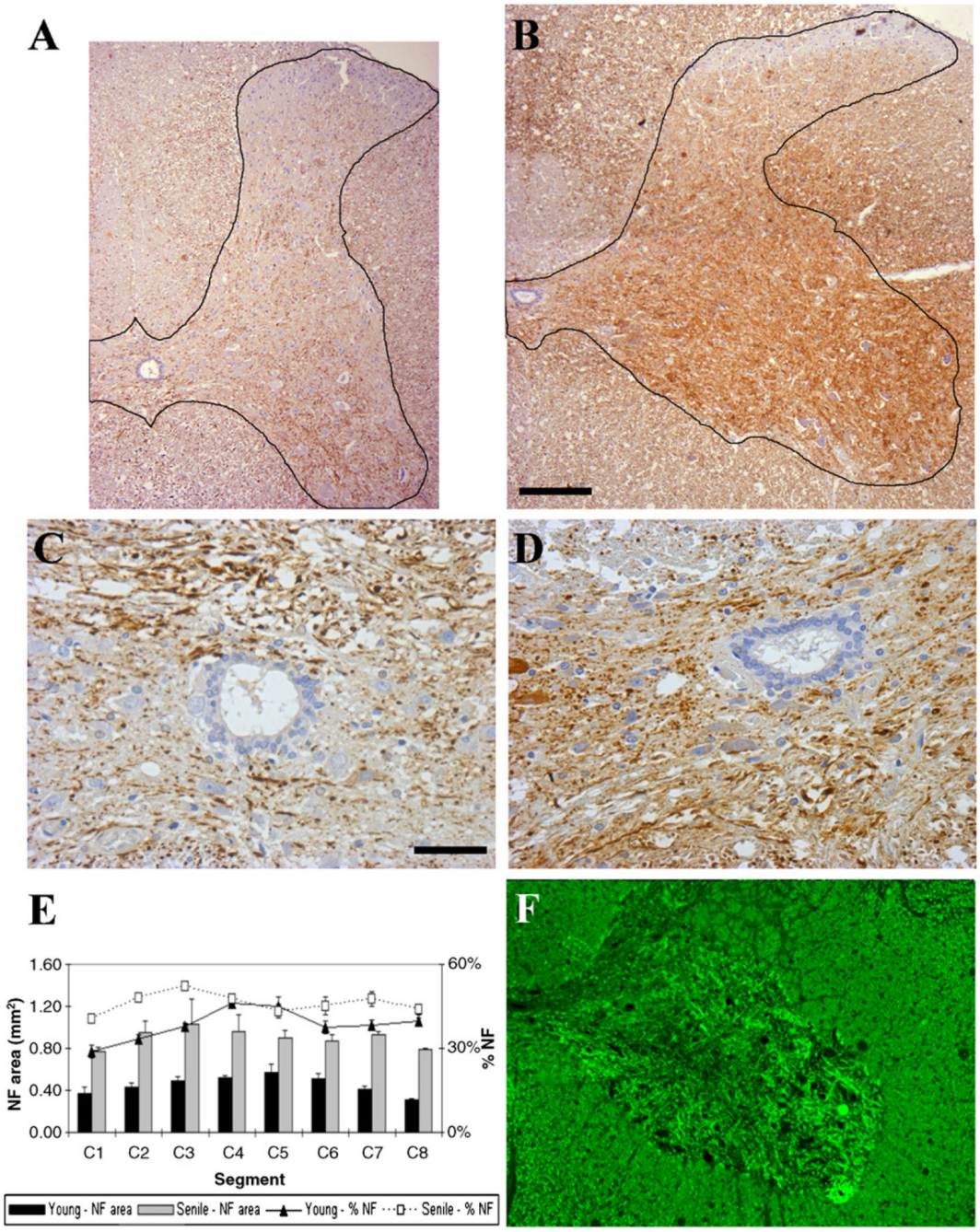

Fig. 2. NF expression during aging

(A) and (B) Show a low magnification view of a hemi C6 segment of a young (A) and a senile (B) rats. It can be seen that NF are distributed throughout the laminas except at the level of laminas I and II. At higher magnification it can be seen that although the MOD of each filament is quite similar either in young rats (C) as well as in senile animal (D) the staining intensity (NF density) of the latter is increased. Differences were statistically significant when we compared the NF density as well as the percentage of NF in relation to the gray matter area (E). (F) A fluorescence staining of NF in a senile C5 segment ventral horn where in the graymatter are seen as thin filaments an in the white matter are points indicating a cross-section of axons. Bar for (A, B, F) = 0.2 mm. Bar for (C, D) = 50 μm.

NIH-PA Author Manuscript

NIH-PA Author Manuscript

NIH-PA Author Manuscript

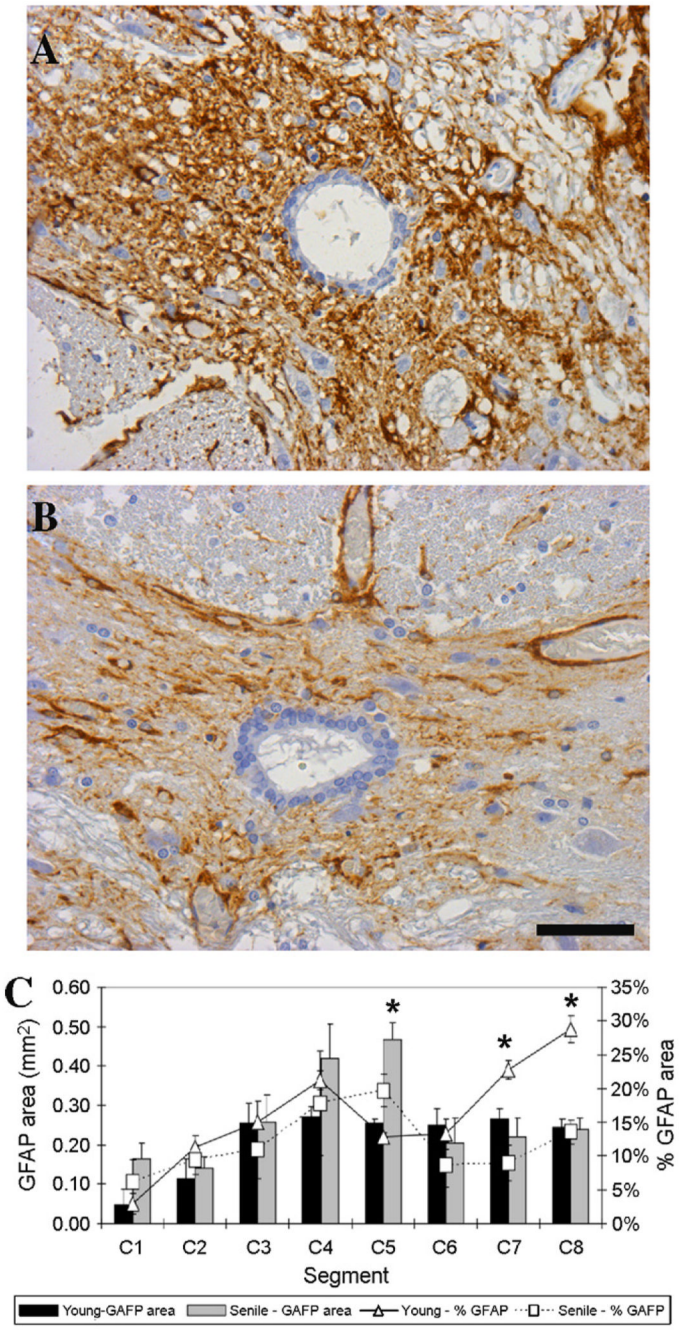

Fig. 3. GFAP expression during aging

There was a clear increase in the MOD of astrocyte immunostaining for GFAP in young (A) as compared to senile animals (B). No ependymal cells area stained. Graph (C) shows that the GFAP area increased significantly only in C5 and that there was a reduction in the percentage of GFAP stained area in relation to the entire gray matter with age. *Significant difference. Bar for (A, B) = 50 μm.

NIH-PA Author Manuscript
NIH-PA Author Manuscript
NIH-PA Author Manuscript

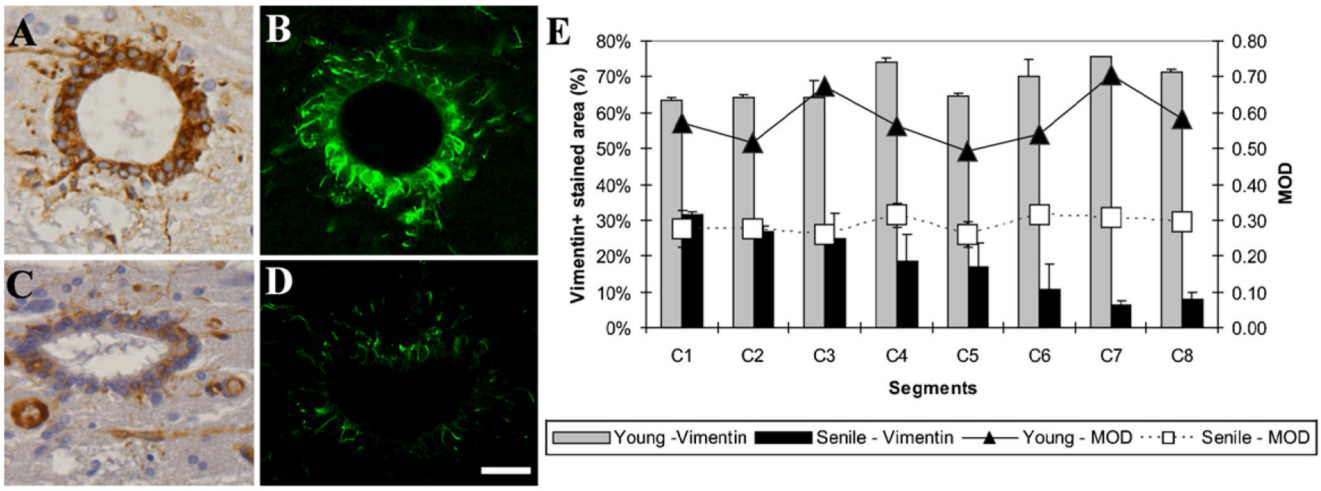

Fig. 4. Vimentin expression during aging

The expression of vimentin was mainly localized in the central canal, although it was also observed in some glial cells and surrounding the blood vessels either in young (A) and senile (C) rats. It can be seen that the density of staining and the MOD decrease in the latter. These differences were statistically significant (E). Fluorescence images at both ages (B, D) show the same pattern as with IHC for the central canal. Bar for (A–D) = 25 μm.

NIH-PA Author Manuscript

NIH-PA Author Manuscript

NIH-PA Author Manuscript

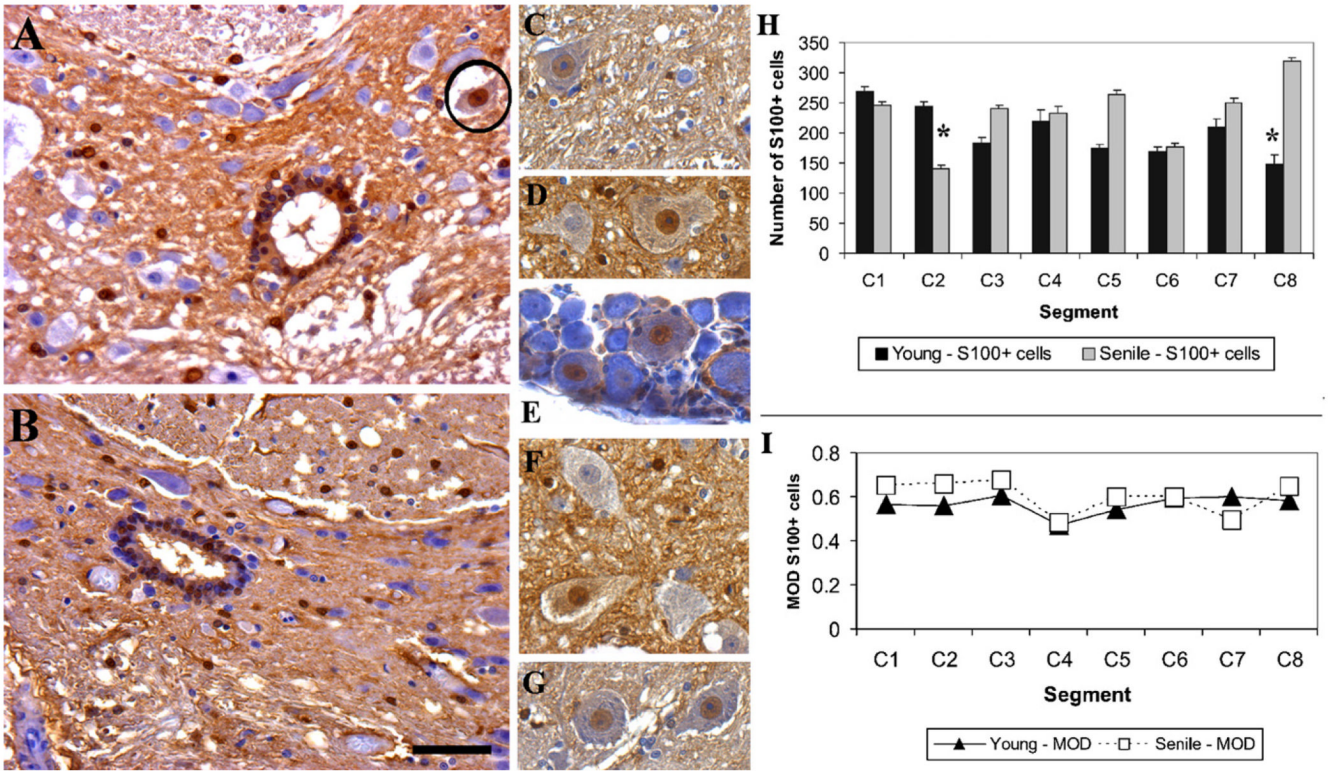

Fig. 5.

S100 expression during aging. Panels (A) and (B) show the ependymal region and lamina X of young and senile rats, respectively, immunostained for the S100 marker. In both cases it can be seen that glial cells of the gray and white matter are stained. Also, in both cases some ependymal cells are stained as well. Panel (A) also shows a neuron and its stained nucleus (encircled cell). This pattern was also observed in some motoneurons both in young (C, D) and senile (F, G) rats. Some neurons of the sensory ganglia are also stained (E). The number of S100+ cells varied in the different segments (H) showing significant differences (*) at C2 and C8. In neither case differences in the MOD were significant (I). Bar for (A–G) = 50 μm.